



Tree Physiology 36, 179–192
doi:10.1093/treephys/tpv117



Research paper

Leaf gas exchange performance and the lethal water potential of five European species during drought

Shan Li¹, Marion Feifel¹, Zohreh Karimi^{1,2}, Bernhard Schuldt³, Brendan Choat⁴ and Steven Jansen^{1,5}

¹Institute for Systematic Botany and Ecology, Ulm University, D-89081 Ulm, Germany; ²Department of Biology, Faculty of Science, Golestan University, 36154 Gorgan, Iran; ³Plant Ecology, Albrecht von Haller Institute for Plant Sciences, University of Göttingen, D-37077 Göttingen, Germany; ⁴University of Western Sydney, Hawkesbury Institute for the Environment, Richmond, NSW 2753, Australia; ⁵Corresponding author (steven.jansen@uni-ulm.de)

Received April 30, 2015; accepted October 5, 2015; published online November 27, 2015; handling Editor Roberto Tognetti

Establishing physiological thresholds to drought-induced mortality in a range of plant species is crucial in understanding how plants respond to severe drought. Here, five common European tree species were selected (*Acer campestre* L., *Acer pseudo-platanus* L., *Carpinus betulus* L., *Corylus avellana* L. and *Fraxinus excelsior* L.) to study their hydraulic thresholds to mortality. Photosynthetic parameters during desiccation and the recovery of leaf gas exchange after rewatering were measured. Stem vulnerability curves and leaf pressure–volume curves were investigated to understand the hydraulic coordination of stem and leaf tissue traits. Stem and root samples from well-watered and severely drought-stressed plants of two species were observed using transmission electron microscopy to visualize mortality of cambial cells. The lethal water potential (ψ_{lethal}) correlated with stem P_{99} (i.e., the xylem water potential at 99% loss of hydraulic conductivity, PLC). However, several plants that were stressed beyond the water potential at 100% PLC showed complete recovery during the next spring, which suggests that the ψ_{lethal} values were underestimated. Moreover, we observed a 1 : 1 relationship between the xylem water potential at the onset of embolism and stomatal closure, confirming hydraulic coordination between leaf and stem tissues. Finally, ultrastructural changes in the cytoplasm of cambium tissue and mortality of cambial cells are proposed to provide an alternative approach to investigate the point of no return associated with plant death.

Keywords: cambium vitality, embolism resistance, hydraulic failure, leaf turgor, photosynthesis, plant death, xylem water potential.

Introduction

Xylem sap in transpiring plants is typically under tension according to the cohesion–tension theory (Dixon and Joly 1895, Tyree 2003a). The cohesive force of the water column in xylem conduits is quantified in vulnerability curves, which show the relationship between xylem water potential (ψ_x , MPa) and the percentage loss of hydraulic conductivity due to embolism formation (PLC %; Tyree et al. 2003, Cochard et al. 2008, 2013). One could expect that with more severe and frequent drought events ψ_x may become more negative, resulting in higher amounts of embolized conduits and higher levels of PLC than under well-watered conditions. A decline in hydraulic conductivity would have potential effects on reducing photosynthesis, transpiration and stomatal conductance (Sperry 2000, Hubbard

et al. 2001, Miyashita et al. 2005), therefore affecting plant growth and productivity (Tyree 2003b, Brodribb 2009). A continued decline of hydraulic conductivity could eventually lead to hydraulic failure of the water transport system, with the propagation of xylem embolism reaching a point of no return from which the plant is unable to recover (Nardini et al. 2013). During severe drought, hydraulic failure can result in complete desiccation of plant tissues and organs (Hoffmann et al. 2011), and induce partial or complete plant mortality (Anderegg 2015).

Considerable attention has been focused on the resistance of plants to xylem hydraulic failure (Hartmann et al. 2015), mostly including hydraulic parameters at the stem level, such as xylem embolism resistance (Lopez et al. 2005), xylem hydraulic safety margins (Choat et al. 2012), sapwood capacitance (Scholz et al. 2014) and sapwood water storage (Pineda-García et al.

2013). However, as a direct indicator of hydraulic resistance to plant death, the lethal water potential (ψ_{lethal}), i.e., the water potential corresponding to the point of no recovery, has been investigated in a small number of species thus far. Lethal water potential of five angiosperm species corresponded to P_{88} (ψ_x at 88% stem PLC; Urli et al. 2013), and ψ_{lethal} of poplar and beech seedlings were related to P_{90} (ψ_x at 90% stem PLC; Barigah et al. 2013a). In contrast, ψ_{lethal} of four gymnosperm species were associated with P_{50} (ψ_x at 50% stem PLC; Brodribb and Cochard 2009). This divergence between angiosperm and gymnosperm tree species is associated with xylem anatomical differences, and various contrasting traits, such as phenology, growth allometry and competition sensitivity (Carnicer et al. 2013).

At the leaf level, stomatal closure is a crucial protective strategy against xylem hydraulic failure (Brodribb and Holbrook 2004, Choat et al. 2007, Chen et al. 2010). In general, plants can be separated into two major groups based on their stomatal control strategy during drought stress: isohydric plants maintain a relatively stable daytime leaf water potential (ψ_l , MPa) under mild and moderate drought conditions by closing their stomata gradually to reduce gas exchange and water loss (Kumagai and Porporato 2012, Sade et al. 2012). In contrast, anisohydric plants tolerate a decline in ψ_l by keeping stomata open to enable continuous gas exchange within certain levels of water stress (Tardieu and Simonneau 1998). Nevertheless, evidence suggests that stomatal closure for both isohydric and anisohydric plants is coordinated with xylem embolism (Sperry and Pockman 1993, Salleo et al. 2000, Meinzer et al. 2009; Manzoni et al. 2014), although this coordination varies to some degree across species (Bond and Kavanagh 1999). For instance, most studies illustrate that ψ_x at stomatal closure ($\psi_{\text{gs,e}}$, MPa) scales with ψ_x at the onset of xylem embolism (P_e , MPa; Nardini et al. 2001, Cochard et al. 2002). Some studies, however, suggest a much closer relationship between $\psi_{\text{gs,e}}$ and P_{50} than P_e (Sparks and Black 1999, Martorell et al. 2014).

Stomatal closure is generally assumed to be the first protective mechanism against drought stress (Tyree et al. 1998). However, the structural threshold to drought-induced tree mortality is not clear. At the tissue level, meristematic tissue such as cambium determines tree growth by producing new layers of xylem and phloem (Liphschitz and Lev-Yadun 1986, Rossi et al. 2013), which allows woody plants to replace dysfunctional cells and to facilitate secondary growth. Previous work showed that the cambium is highly resistant to leaf defoliation in *Abies balsamea* seedlings (Rossi et al. 2009b), and is the last resilient tissue to dehydration in *Populus nigra* seedlings (Barigah et al. 2013b). These results suggest that cambium vitality can be a useful indicator of tree growth and also mortality (Gričar et al. 2014). Nevertheless, the majority of studies on cambium focused on seasonal changes of cambium activity (Farrar and Evert 1997, Fuchs et al. 2010), or quantification of cambium cells with different irrigation regimes (Abe et al. 2003, Rossi

et al. 2009a, de Luis et al. 2011, Balducci et al. 2013). Research on the ultrastructure of cambial cells in relation to plant death remains surprisingly limited (Thomas 2013).

In this study, we aimed to estimate ψ_{lethal} of five angiosperm tree species and expected that these values would be closely related to stem P_{88} values. We applied drought-stress rehydration experiments on seedlings of the species studied and quantified the dynamics of photosynthesis and transpiration during the drought and rewatering period to estimate ψ_{lethal} . We defined a moderate stress level as ψ_m (midday leaf water potential) less negative than P_{50} , while severe water stress was considered to have ψ_m between P_{50} and P_{88} . Death was predicted to occur at ψ_m values that were more negative than P_{88} . We also hypothesized that there is a coordination of $\psi_{\text{gs,e}}$ and P_e for the five tree species selected. We conducted stomatal response curves, leaf pressure–volume (PV) curves and stem vulnerability curves to test the hydraulic coordination between leaf and stem organs. In addition, we hypothesized that cambium would suffer cellular failure at the time of plant death in both stem and root organs.

Materials and methods

Plant material

The following five European angiosperm species were selected: *Acer campestre* L., *Acer pseudoplatanus* L., *Carpinus betulus* L., *Corylus avellana* L. and *Fraxinus excelsior* L. Seedlings of these species were used for a drought experiment. These seedlings were 2–4 years old and 30–90 cm tall. In November 2013, samples belonging to the same population of plants were bought from a local nursery (Kordes Jungpflanzen Handels GmbH, Bilsen, Germany), and transported to the Botanical Garden of Ulm University (48°25'9.84" N, 9°57'59.759" E). The seedlings were transferred to 3-l pots, with a composition of 50% organic soil, 20% sand, 20% loam and 10% turf. In spring and early summer 2014, all seedlings were well-watered on a daily basis and pesticides were applied twice to avoid insect herbivory.

Branches from adult trees grown in the Botanical Garden of Ulm University were used for stem vulnerability curves and leaf PV curves. All branches were ~2–5 years old and from the same five species selected for the drought experiment. The adult trees at Ulm University were from the same population as the plants from the local nursery. Samples were taken from sun-exposed branches at a height of 2–3 m during early morning in the growing season of 2013 and 2014.

Experimental design

In June 2014, 11–14 healthy seedlings of each species were placed under a rainout shelter (8 × 4 m), which was constructed with a special UV translucent foil (Lumisol clear AF; Folitec, Westerburg, Germany), having a light transmittance of 90% and a UV-B transmittance of 70%. The ground was covered with a foil to avoid as much as possible water uptake from ground

water or rain. In addition, this foil reduced the growth of weeds. The soil was also given a slight inclination to facilitate water runoff. The temperature and humidity was recorded with a data logger (EL-USB-2, Lascar electronics Inc., Salisbury, UK). The average temperature and relative humidity were 17.9 ± 6.5 °C and $75 \pm 20.6\%$, respectively, over the entire duration of the experiment, i.e., from 10 July 2014 to 26 September 2014.

Before starting the drought experiment, plants were well-watered on a daily basis. Overall, the approach applied was based on Brodrigg and Cochard (2009) and Urli et al. (2013). For a list of the physiological parameters described below, acronyms and their definitions, see Table 1. A Li-Cor 6400 XT portable photosynthesis system (LI-COR, Lincoln, NE, USA) was used to measure the maximum CO₂ assimilation rate (A_{\max} , $\mu\text{mol CO}_2 \text{ m}^{-2} \text{ s}^{-1}$), transpiration rate (E_{\max} , $\text{mmol H}_2\text{O m}^{-2} \text{ s}^{-1}$) and stomatal conductance ($g_{s \max}$, $\text{mol H}_2\text{O m}^{-2} \text{ s}^{-1}$). The LED red and blue light source was set to a fixed intensity of $1200 \mu\text{mol m}^{-2} \text{ s}^{-1}$. Other parameters included a $400 \mu\text{mol mol}^{-1}$ reference CO₂ concentration, 20 °C block temperature and

$500 \mu\text{mol s}^{-1}$ pump flow rate. The A_{\max} , E_{\max} and $g_{s \max}$ were measured on three mature 3- to 5-month-old leaves for each plant. These leaves were labelled to repeat similar measurements over time. Photos were taken from leaves smaller than the Li-Cor leaf chamber to estimate the leaf area measured. Five individuals from each species were randomly selected to measure ψ_m , with three leaves being measured on a single plant. Leaves were bagged with aluminium bags for at least 1 h before midday to reach equilibrium between ψ_l with ψ_x , and ψ_m was measured using a Scholander pressure chamber (PMS Instrument Company, Albany, OR, USA).

Drought was induced by withholding water from the plants over a variable number of days, ranging from 7 to 56 days. The plants were water-stressed to different levels based on the ψ_m measurements obtained. In general, we aimed for moderate and severe levels of water stress, as well as lethal doses of drought. Midday leaf water potential was measured on one to three leaves from each plant with the Scholander pressure chamber every 1–3 days. For each plant, measurements of A , E and g_s

Table 1. Acronyms and units of the parameters measured in this study with their corresponding definitions.

Acronyms	Units	Definitions
A	$\mu\text{mol CO}_2 \text{ m}^{-2} \text{ s}^{-1}$	CO ₂ assimilation rate
A_{\max}	$\mu\text{mol CO}_2 \text{ m}^{-2} \text{ s}^{-1}$	Maximum CO ₂ assimilation rate
E	$\text{mmol H}_2\text{O m}^{-2} \text{ s}^{-1}$	Transpiration rate
E_{\max}	$\text{mmol H}_2\text{O m}^{-2} \text{ s}^{-1}$	Maximum transpiration rate
g_s	$\text{mol H}_2\text{O m}^{-2} \text{ s}^{-1}$	Stomatal conductance rate
$g_{s \max}$	$\text{mol H}_2\text{O m}^{-2} \text{ s}^{-1}$	Maximum stomatal conductance rate
PLC	%	Percentage loss of hydraulic conductivity
PLC _A	%	PLC corresponding to ψ_{lethalA}
PLC _E	%	PLC corresponding to ψ_{lethalE}
PLC _{gs}	%	PLC corresponding to ψ_{lethalgs}
P_e	MPa	ψ_x at the onset of xylem embolism
P_{50}	MPa	ψ_x at 50% PLC
P_{88}	MPa	ψ_x at 88% PLC
RWC _{tip}	%	Relative water content at turgor loss point
S_{A50}		Slope of the tangent drawn through the midpoint of the A response curve
S_{E50}		Slope of the tangent drawn through the midpoint of the E response curve
S_{gs50}		Slope of the tangent drawn through the midpoint of the g_s response curve
S_{P50}		Slope of the tangent drawn through the midpoint of the stem vulnerability curve
$t_{1/2}$	days	Number of days for A , E and g_s to recover to more than half of the maximum values
Ψ_{Ae}	MPa	ψ_x at the cessation of photosynthesis
Ψ_{Ee}	MPa	ψ_x at the cessation of transpiration
$\Psi_{gs e}$	MPa	ψ_x at stomatal closure
Ψ_{gs50}	MPa	ψ_x at 50% of maximum stomatal conductance
Ψ_l	MPa	Leaf water potential
Ψ_{lethal}	MPa	Xylem lethal water potential
Ψ_{lethalA}	MPa	Xylem lethal water potential calculated based on A
Ψ_{lethalE}	MPa	Xylem lethal water potential calculated based on E
Ψ_{lethalgs}	MPa	Xylem lethal water potential calculated based on g_s
Ψ_m	MPa	Midday leaf water potential/midday xylem water potential
Ψ_x	MPa	Xylem water potential
π_{tip}	MPa	ψ_l at turgor loss point
ϵ		Modulus of elasticity
π_o	MPa	Osmotic potential at full turgor

were based on the three leaves that were labelled and measured previously. All Li-Cor measurements were conducted from 9 am to 1 pm and were repeated every 2–3 days. Given considerable fluctuation in light intensity and temperature during the 4 h of measurements, all plants were measured in a fixed order, which means that temporal differences for individual plants were kept as minimal as possible. In case leaves selected for our Li-Cor measurements dropped off, additional, fully developed leaves were used to take measurements.

Once the A , E and g_s values were lower than 50% of A_{\max} , E_{\max} and $g_{s\max}$ for each specific plant and the required ψ_m was targeted, plants were rewatered daily during the late afternoon or early evening until the soil was fully saturated. Photosynthetic recovery was then measured in the morning on a daily basis until values were higher than 50% of the maximum. In case a particular plant showed slow recovery, Li-Cor measurements were not conducted daily, but every 2–3 days. The number of days for A , E and g_s to recover to more than half of the maximum values ($t_{1/2}$, days⁻¹) were counted. For some plants, $t_{1/2}$ was estimated by applying a linear regression of the data, especially when the exact recovery day was missed. Lethal water potential was calculated by plotting ψ_m against $1/t_{1/2}$ (Brodrribb and Cochard 2009, Brodrribb et al. 2010), which was done for A , E and g_s (Urli et al. 2013). After the experiment, all plants were watered on a daily basis, including the plants that showed no photosynthetic recovery. We then determined survival of the severely desiccated plants in April 2015 by noting whether or not there was leaf flushing.

Embolism resistance of stem xylem

In late May 2013 and 2014, four to eight branches from at least five specimens per species that were ~5 years old were collected in the morning. Branches were immediately wrapped in wet towels and dark plastic foil to prevent dehydration. The samples were then transported to Göttingen University and embolism resistance was measured within 5 days using the Cavitron technique (Cochard et al. 2005). Stems were connected to a Xyl'em apparatus (Bronkhorst, Montigny les Cormeilles, France) for determining the maximum hydraulic conductivity at 6 kPa, interrupted by three 10-min flushes at 120 kPa to remove potential emboli. Subsequently, branch samples of 27.5 cm length were mounted in a custom-built rotor chamber of the Cavitron, which uses a commercially available centrifuge as basis (Sorvall RC-5C, Thermo Fisher Scientific, Waltham, MA, USA), and spun at defined velocities as recorded with the CaviSoft programme (version 2.1, University of Bordeaux, Bordeaux, France) to generate stem vulnerability curves. For all hydraulic measurements we used demineralized, filtered (0.2 μm) and degassed water, to which 10 mM KCl and 1 mM CaCl₂ were added.

For *F. excelsior*, the maximum vessel length based on air injection was ~1.0–1.2 m, which exceeded the sample length of the Cavitron (Cochard et al. 2005). Therefore, the bench dehydration

technique was used to construct stem vulnerability curves for this species. Eight 1.5–2 m long sun-exposed branches were collected from five adult trees in the Botanical Garden of Ulm University, immediately brought to the laboratory, re-cut under water, and then dehydrated in the laboratory with different time intervals ranging from 1 to 24 h (Wang et al. 2014). After bagging up the plant material for 1 h to obtain equilibrium between ψ_l and stem ψ_x , three leaves attached to the current year stem were measured for ψ_l . Branches were then rehydrated in water for half an hour to eliminate cutting artefacts, and were then recut under water several times into 7–10 cm long current year stem segments (Wheeler et al. 2013, Torres-Ruiz et al. 2015). These final segments were used to take PLC measurements with a Sperry apparatus:

$$\frac{\text{PLC}}{100} = \frac{K_{\max} - K_h}{K_{\max}}, \quad (1)$$

with K_h (kgs⁻¹ m MPa⁻¹) representing the hydraulic conductivity of the stems under different water potential before being flushed with degassed and distilled water, and K_{\max} (kgs⁻¹ m MPa⁻¹) representing the hydraulic conductivity of the same stems after being flushed.

PV curves

In August 2013, three branches that were 2–5 years old were collected in the early morning. The samples were cut off at a height of 2–3 m from three different adult trees per species growing in the Botanical Garden of Ulm University. They were put into bags filled with wet tissue and immediately brought to the laboratory. Three mature leaves per species were selected to generate leaf PV curves. Briefly, the initial ψ_l was measured using a Scholander pressure chamber and the fresh weight was measured using a balance. Then, the leaves were bench dried for several hours while ψ_l and the corresponding drop in weight were measured until ψ_l had dropped to about –3 MPa. Finally, the leaves were put into the oven at >70 °C for at least 2 days and their dry mass was measured. The leaf PV curves obtained were then used to calculate the osmotic potential at full turgor (π_o), ψ_l at the turgor loss point (π_{tlp}), the modulus of elasticity (ϵ) and the relative water content at the turgor loss point (RWC_{tlp}; Sack and Pasquetl-Kok 2011).

Transmission electron microscopy

Stem and root material from *C. avellana* and *C. betulus* was tested for cambium vitality of both organs. We selected these two species as they belong to the same family and are both diffuse porous species, with *C. betulus* being resistant to embolism while *C. avellana* was more vulnerable to embolism ($P_{50} = -3.79$ and -2.09 MPa, respectively). For both species, we selected a well-watered control plant and a plant that was exposed to drought stress for ~1 month. We assumed that the drought-stressed plants, which had all their leaves wilted and ψ_m around

ψ_{lethal} , were dead. The drought-stressed plant of *C. avellana* was stressed for ~10 days longer than the time required to reach ψ_{lethal} for this species. The *C. betulus* seedling, however, was stressed for a shorter period than the average period needed to reach ψ_{lethal} . Stem and root cambium samples (~2 mm³) from well-watered and severely wilted plants were collected on 9 September 2014 from the main stem (~3 cm above the soil) and the main root (~2 cm below ground). The samples were immediately fixed in a standard solution (2.5% glutaraldehyde, 0.1 mol phosphate, 1% saccharose, pH 7.3). Further transmission electron microscopy (TEM) preparation followed a standard protocol (Scholz et al. 2013). Ultra-thin transverse sections were observed with a JEOL 1400 TEM (JEOL Ltd., Tokyo, Japan) and ImageJ (version 1.48v, National Institutes of Health, Bethesda, MD, USA) was applied to measure the cambial cell wall thickness.

Statistics

A sigmoidal function was used in Matlab (version R2013b, MathWorks, Natick, MA, USA) to fit curves for A , E and g_s data versus ψ_m (Brodribb and Cochard 2009). For each species, the average values of A_{max} , E_{max} and $g_{s \text{ max}}$ based on the measurements from all well-watered individual plants were used to manually fix the starting points of the curves near the y -intercept:

$$y = \frac{a}{(1 + \exp(-(x - x_0)/b))}, \quad (2)$$

with x (MPa) representing the absolute value of ψ_m , y representing the photosynthetic parameters (A , E and g_s), and a , b , x_0 being constants.

Table 2. Summary of physiological parameters measured in five angiosperm species. Material from seedlings was used for measurements of A , E and g_s , while stem vulnerability curves and PV curves were conducted on tree branches with a similar age as the seedlings. Standard deviations (SD) were given for the parameters extracted from three PV curves, but were not available for the other parameters as the data collected were combined into a single curve. Acronyms and units follow the definitions shown in Table 1.

Measurements	Parameters	<i>A. campestre</i>	<i>A. pseudoplatanus</i>	<i>C. avellana</i>	<i>C. betulus</i>	<i>F. excelsior</i>
Vulnerability curve	P_{50}	-4.80	-2.99	-2.09	-3.79	-2.72
	P_{88}	-5.33	-4.13	-2.77	-4.43	-3.75
	P_e	-4.15	-1.75	-1.33	-3.02	-1.60
	S_{P50}	0.77	0.40	0.66	0.65	0.44
A	A_{max}	12.97	10.62	7.85	11.12	12.26
	ψ_{Ae}	-3.37	-1.44	-1.67	-3.27	-2.94
	S_{A50}	-4.45	-13.48	-12.13	-4.06	-5.09
g_s	$g_{s \text{ max}}$	0.22	0.17	0.14	0.16	0.22
	ψ_{gse}	-3.24	-1.27	-1.35	-3.57	-2.66
	ψ_{gs50}	-1.89	-0.97	-1.24	-2.18	-1.55
	S_{gs50}	-0.08	-0.27	-0.65	-0.06	-0.10
E	E_{max}	1.87	1.55	1.44	1.51	2.31
	ψ_{Ee}	-3.19	-1.39	-1.33	-3.39	-2.72
	S_{E50}	-0.93	-2.04	-6.84	-0.71	-1.03
PV curve	π_{tip}	-1.87 ± 0.17	-1.75 ± 0.14	-1.85 ± 0.65	-2.33 ± 0.07	-2.08 ± 0.18
	ϵ	7.43 ± 0.16	8.02 ± 2.14	4.57 ± 2.11	17.02 ± 7.81	9.51 ± 2.78
	π_o	-1.55 ± 0.07	-1.47 ± 0.11	-1.39 ± 0.46	-1.87 ± 0.17	-1.74 ± 0.11
	RWC _{tip}	78.19 ± 1.26	77.97 ± 6.35	61.68 ± 15.54	86.91 ± 4.99	78.81 ± 9.37

A_e , E_e and $g_{s \text{ e}}$ were calculated as the x intercepts of tangents drawn through the midpoint of the fitted curves, and referred to ψ_x at the cessation of photosynthesis, transpiration and stomatal closure, respectively. The slopes of the tangents for these curves (S_{A50} , S_{E50} and S_{gs50} ; Table 1) were also derived from this function.

The following Weibull function (Cai et al. 2014) was used to fit the stem vulnerability curves in Matlab, to determine P_{50} , P_{88} and S_{P50} . P_e was calculated as the x intercept of a tangent drawn through the midpoint of the following Weibull curve (Meinzer et al. 2009):

$$\text{PLC} = 100 \times \left(1 - e^{-\left(\frac{T}{b}\right)^c} \right) \quad (3)$$

with T representing the tension of the Cavatron (MPa), and b and c being Weibull constants.

Linear regression analysis was performed in Excel (Microsoft, Redmond, WA, USA) to calculate ψ_{lethal} and to evaluate the relationship between different parameters.

Results

Stem vulnerability curves and leaf photosynthetic dynamics during drought

There was considerable variation in the stem vulnerability curves of the five species (Table 2; Figure 1). The most embolism vulnerable species was *C. avellana* ($P_{50} = -2.1$ MPa) and the most embolism resistant one was *A. campestre* ($P_{50} = -4.8$ MPa). The stem vulnerability curves could be fitted with the Weibull function

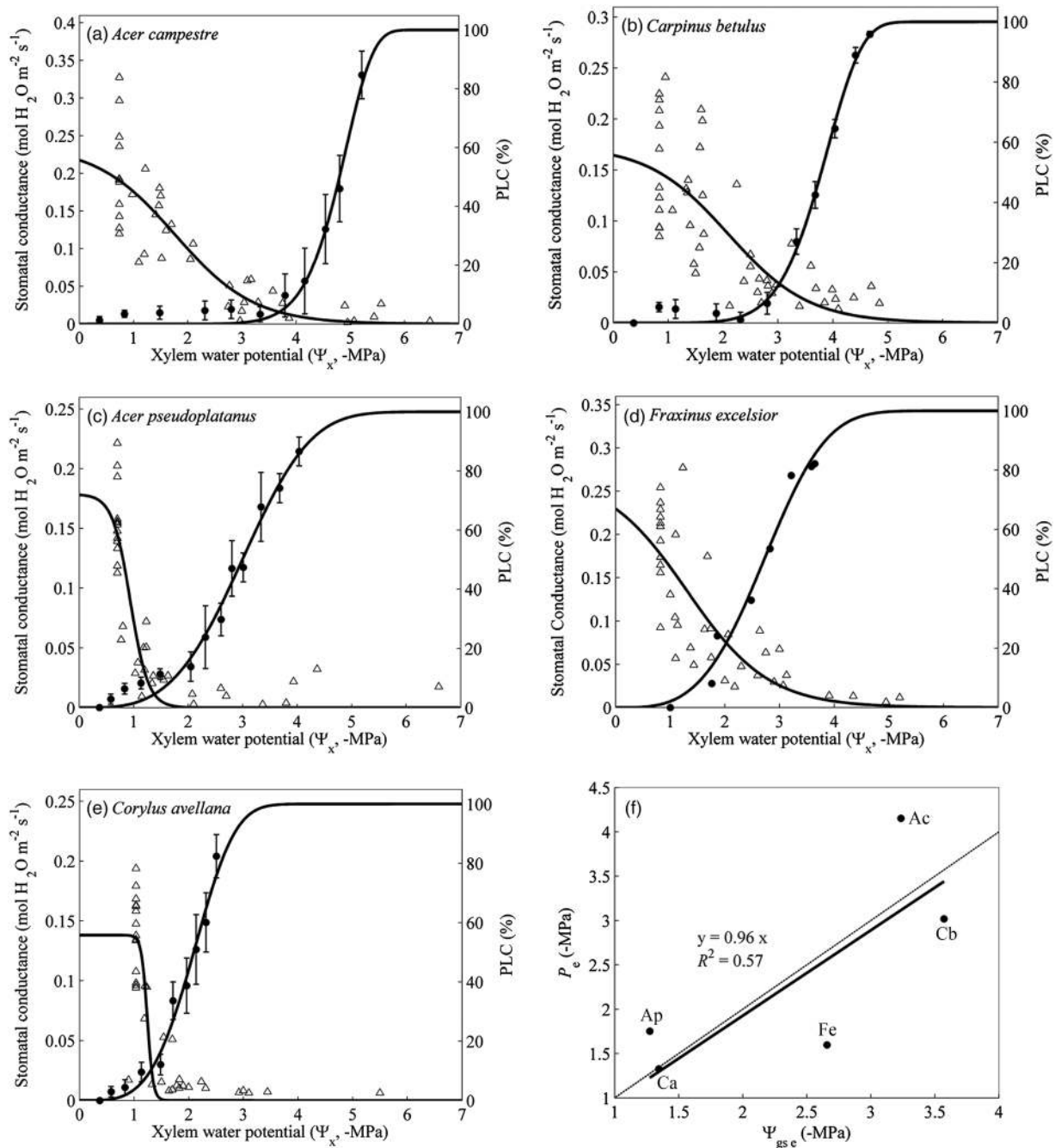


Figure 1. Stem vulnerability curves and stomatal response curves under different midday leaf water potential (ψ_m) for the five species studied (a–e). For stem vulnerability curves, each PLC value (closed circles) is based on the mean value \pm SD from four to eight stems, except for *F. excelsior* (d), where one point is collected from one stem segment. Each point (triangles) in the stomatal response curves is the mean value of three measurements from a single leaf. The regression between the xylem water potential at stomatal closure (ψ_{gs_e}) and the xylem water potential at the onset of embolism (P_e) is shown in (f). This regression line was forced to go through the origin and the grey line represents the 1 : 1 line. Ac, *Acer campestre*; Ap, *Acer pseudoplatanus*; Ca, *Corylus avellana*; Cb, *Carpinus betulus* and Fe, *Fraxinus excelsior*.

(root mean square error ≤ 5.4) and all curves were sigmoidal. The start of the stem vulnerability curve of *A. pseudoplatanus*, however, showed PLC values that were slightly higher than the fitted curve (Figure 1c).

Overall, A , E and g_s were significantly correlated with each other ($P < 0.01$). Variation in the photosynthetic response to

different levels of drought was observed in the five species (Figure 1; Table 2), which was also clearly based on variation in S_{A50} , S_{E50} and S_{g50} values (Table 2). Furthermore, embolism-resistant species such as *A. campestre* and *C. betulus* showed higher photosynthetic capacity, while more embolism vulnerable species (i.e., *C. avellana* and *A. pseudoplatanus*) showed lower

photosynthetic levels. However, statistical analysis showed no significant linear regression between A_{\max} and P_{50} ($R^2 = 0.57$, $P = 0.14$), E_{\max} and P_{50} ($R^2 = 0.01$, $P = 0.86$) and $g_{s\max}$ and P_{50} ($R^2 = 0.33$, $P = 0.31$).

Stomatal response to drought and leaf turgor

Acer pseudoplatanus and *C. avellana* were considered to be isohydric as g_s decreased dramatically within a small range of ψ_m , which was also shown by more negative S_{gs50} values compared with the other species (Table 2). *Fraxinus excelsior*, *A. campestre* and *C. betulus* were anisohydric. They were found to tolerate a declining ψ_m with a slow reduction of gas exchange (Figure 1). The anisohydric stomatal behaviour of these species was also reflected in their high (i.e., close to zero) S_{gs50} values.

Acer pseudoplatanus, *C. avellana* and *F. excelsior* had less negative P_e values than *A. campestre* and *C. betulus*. The former three species also had less negative A_e , E_e and $\psi_{gs\ e}$ values than the latter two. There was a weak and non-significant 1 : 1 correlation between $\psi_{gs\ e}$ and P_e across the five species ($R^2 = 0.57$, $P = 0.14$; Figure 1f). A similar but significant relationship was found between A_e and P_e ($R^2 = 0.55$, $P = 0.002$). There was also no significant correlation between $g_{s\ e}$ and P_{50} ($R^2 = 0.2$, $P = 0.15$), $\psi_{gs\ 50}$ and P_{50} ($R^2 = 0.45$, $P = 0.22$) and between E_e and P_e ($R^2 = 0.57$, $P = 0.14$).

Moreover, there was a linear, non-significant relationship between $\psi_{gs\ e}$ and π_{tip} ($R^2 = 0.56$, $P = 0.14$; Figure 2), which was different from the 1 : 1 relationship. A positive relationship between $\psi_{gs\ 50}$ (ψ_m corresponding to 50% stomatal closure) and π_{tip} was found ($R^2 = 0.63$, $P = 0.11$). Both relationships suggested that stomatal closure and leaf turgor were coordinated.

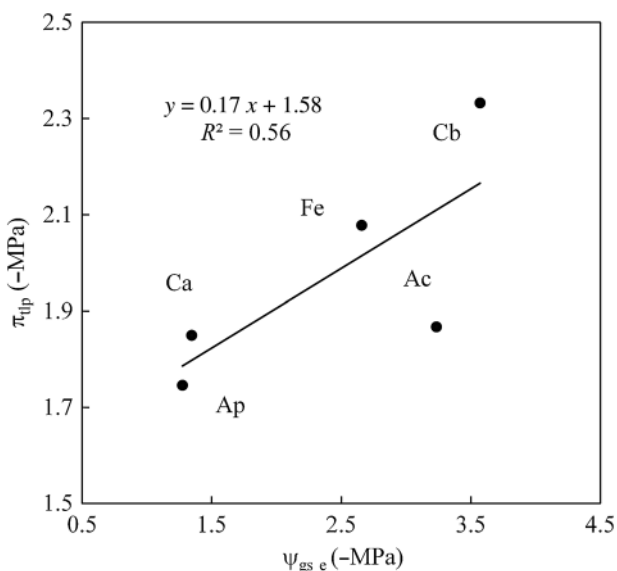


Figure 2. Linear regression between the xylem water potential at stomatal closure ($\psi_{gs\ e}$) and leaf water potential at turgor loss point (π_{tip}). Ac, *Acer campestre*; Ap, *Acer pseudoplatanus*; Ca, *Corylus avellana*; Cb, *Carpinus betulus*; Fe, *Fraxinus excelsior*.

There was no relationship between P_{50} and π_o (osmotic potential at full turgor; $R^2 = 0.04$, $P = 0.74$).

Lethal water potential

In general, the seedlings of all species showed relatively quick recovery (<9 days) under moderate water stress, and relatively slow recovery (up to 18 days) or recovery failure after severe water stress. Similar recovery trends were found for E , A and g_s , although there were minor differences in the recovery time $t_{1/2}$. The relationship between $1/t_{1/2}$ and ψ_m based on E had the best fit compared with A and g_s . Therefore, E was the best indicator to estimate ψ_{lethal} for the five species studied.

The relationship between $t_{1/2}$ as based on E values and ψ_m could be fitted with a linear regression for all species. Both *C. avellana* and *F. excelsior* had low fitting probability ($R^2 = 0.29$, $P = 0.08$ and $R^2 = 0.36$, $P = 0.04$, respectively; Figure 3a–e). There were intraspecific differences in $t_{1/2}$ among the plants stressed to similar ψ_m . For example, $t_{1/2}$ of two *C. avellana* seedlings with ψ_m at -2.9 and -3 MPa were 11 and 7 days, respectively. All five species were able to recover to half of the E_{\max} overnight, except for *C. betulus*, which required at least 2 days (Figure 3b). However, a few *F. excelsior* seedlings showed quick recovery of E overnight for ψ_m values from -1.75 to -3.91 MPa.

The average ψ_{lethal} of the five tree species ranged from -4.39 ± 0.26 to -6.06 ± 0.47 MPa, which corresponded to PLC values between 87 and 100%, with minor differences only for A , E and g_s (Table 3). Lethal water potential calculated based on A ($\psi_{lethalA}$), E ($\psi_{lethalE}$) and g_s ($\psi_{lethalgs}$) were positively correlated with embolism resistance of the stem xylem. Specifically, ψ_{lethal} had a linear but non-significant relationship with P_{50} , P_{88} and P_{99} ($R^2 = 0.20$, 0.17 and 0.13 , and $P = 0.45$, 0.49 and 0.58 , respectively). Nevertheless, ψ_{lethal} was closest to P_{99} and the linear regression between both parameters was close to a 1 : 1 relationship when we included data from six additional species from literature ($y = 0.93x + 0.65$, $R^2 = 0.51$, $P = 0.02$).

Two seedlings of *C. avellana* that were water-stressed during 2 weeks showed complete leaf mortality. However, new leaves flushed at the bottom of the stem within a few weeks after rewatering. Moreover, leaf flushing was observed after winter in April 2015 for a total of six seedlings from all five species that were water-stressed beyond ψ_{lethal} (Figure S1 available as Supplementary Data at *Tree Physiology* Online).

Cambium vitality

The fusiform stem cambium cells of the well-watered *C. avellana* and *C. betulus* showed a maximum thickness of 1.59 and 2.23 μm , respectively, and many lipid droplets in a dense cytoplasm (Figure 4a and c). The cell membrane of the cambium cells was closely attached to the cell walls. The cambium cells in a stem sample of *C. avellana* included numerous small vacuoles, protein bodies, an electron dense nucleus and in some cases nucleolus. In *C. betulus*, the cambium showed vacuoles and a

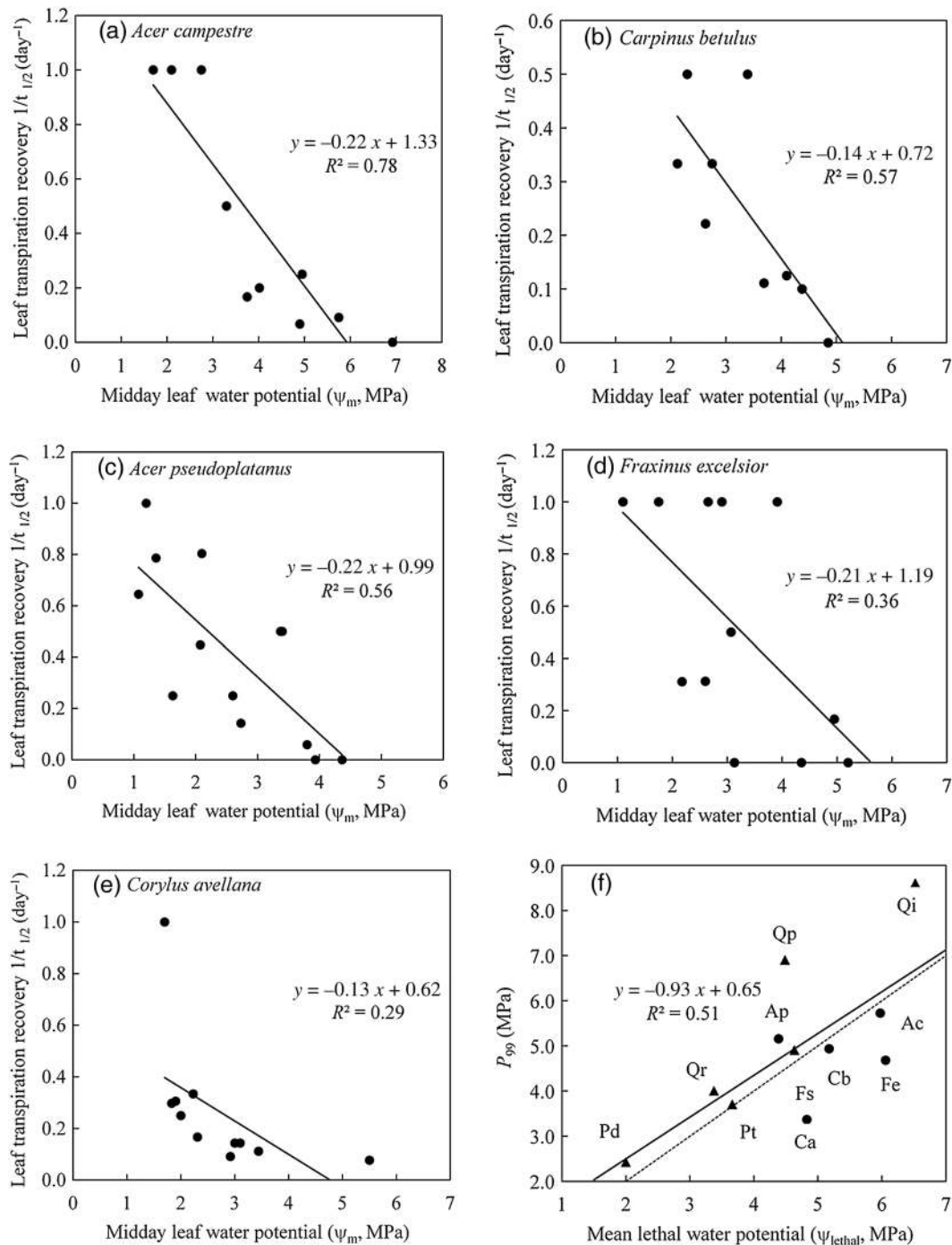


Figure 3. Linear regression between midday leaf water potential (ψ_m) and the reciprocal of the time ($1/t_{1/2}$) required to recover to more than half of the maximum transpiration rate (E_{max}) in five species (a–e). The more negative the plants were water-stressed, the higher the $1/t_{1/2}$ values, except for a few plants from *F. excelsior*. The lethal water potential based on E ($\psi_{lethalE}$) was calculated as the intercept value of the linear regression on the x axis, ranging from -4.4 to -6 MPa. A similar approach was applied to A and g_s to estimate $\psi_{lethalA}$ and $\psi_{lethalg_s}$. The linear regression (f) between the mean lethal water potential (ψ_{lethal} , MPa) and P_{99} was based on five species from this study (closed circles) and six species from the literature (triangles; Barigah et al. 2013a, Urii et al. 2013). Ac, *Acer campestre*; Ap, *Acer pseudoplatanus*; Cb, *Carpinus betulus*; Ca, *Corylus avellana*; Fs, *Fagus sylvatica*; Fe, *Fraxinus excelsior*; Pd, *Populus deltoides* \times *Populus nigra*; Pt, *Populus tremula*; Qi, *Quercus ilex*; Qp, *Quercus petraea*; Qr, *Quercus robur*.

smooth and dense endoplasmic reticulum. No clear ultrastructural differences were noticed between the stem and the root cambium in the well-watered control plants.

The plasmalemma of stem cambium cells in the water-stressed plants was shrunk or ruptured, showing clear leakage

and breakdown of cellular organelles (Figure 4b and d). In *C. avellana*, all fusiform cambium cells were distinctly damaged, showing various empty vesicles, but little or no intact cell organelles. Also, nuclei and nucleoli were not observed in these cells. About 90% of the fusiform cambium cells in *C. betulus* were

Table 3. Lethal water potential (Ψ_{lethal}) of the five species studied based on photosynthesis rate (A), transpiration rate (E) and stomatal conductance (g_s), together with the corresponding PLC values, as well as the mean lethal water potential and PLC values (\pm SD). Standard deviation values are not available for Ψ_{lethal} and the corresponding PLC, which are calculated from single linear regressions shown in Figure 3.

Parameters	<i>A. campestre</i>	<i>A. pseudoplatanus</i>	<i>C. avellana</i>	<i>C. betulus</i>	<i>F. excelsior</i>
$\Psi_{\text{lethal}A}$	-6.09	-4.61	-4.86	-4.40	-6.00
$\Psi_{\text{lethal}E}$	-5.93	-4.46	-4.77	-5.11	-5.62
$\Psi_{\text{lethal}g_s}$	-5.91	-4.09	-4.85	-6.01	-6.56
PLC _A	99.99	95.50	100.00	86.85	100.00
PLC _E	99.87	93.69	100.00	99.72	99.98
PLC _{g_s}	99.84	87.23	100.00	100.00	100.00
Ψ_{lethal}	-5.98 \pm 0.10	-4.39 \pm 0.26	-4.83 \pm 0.05	-5.17 \pm 0.81	-6.06 \pm 0.47
PLC _{lethal}	99.90 \pm 0.08	92.14 \pm 4.35	100.00 \pm 0.00	95.52 \pm 7.51	99.99 \pm 0.01

damaged, while some were still intact. Cambial ray initial cells in this species were more resistant to cell death than fusiform initial cells, i.e., the ray initials remained intact and did not appear to disintegrate (Figure 4e and f). We found similar cambium ultra-structural differences between root and shoot samples for the water-stressed plants, showing that the consequences of drought stress were equally visible at the cambium level in both organs.

Discussion

Seedlings that were drought-stressed to ψ_x values close to 99% stem PLC failed to recover after the drought experiment in 2014 (Table 3). This confirms that angiosperms are more resistant to high levels of PLC than gymnosperms (Brodribb and Cochard 2009). However, plants that were drought-stressed beyond the estimated Ψ_{lethal} showed leaf flushing during next spring, which indicates that Ψ_{lethal} values based on photosynthetic recovery time are underestimated, and that true values of Ψ_{lethal} are likely to be at ψ_x beyond 100% PLC. This finding suggests that lethal levels of drought might be higher than values previously reported (Tyree and Sperry 1988, Tyree et al. 2002, Kursar et al. 2009, Barigah et al. 2013a, Urli et al. 2013), although differences could be due to intraspecific variation, the experimental set up, the age of the plant material, the pot size (Poorter et al. 2012) and micro-environmental conditions. Flushing of new leaves was also reported for *Populus tremula* and *Quercus robur* by Urli et al. (2013). According to the vulnerability segmentation hypothesis (Tyree and Ewers 1991), distal parts of plants such as leaves could be more easily sacrificed than stems and roots. Therefore, leaf mortality and leaf abscission does not equal plant death per se (Lu et al. 2010). Instead, it is a protective mechanism for deciduous plants to cope with severe drought, and to preserve water and nutrients in tissues that remain alive (Griffiths et al. 2014).

The recovery performance of xylem hydraulic conductivity was negatively correlated with embolism resistance under moderate water stress levels in seven temperate tree species (Ogasa et al. 2013). We did not find a significant correlation between

photosynthetic recovery and xylem embolism resistance. However, given the positive correlation between xylem embolism resistance and Ψ_{lethal} , as well as a functional link between plant micromorphology and embolism resistance (Lens et al. 2011, Markesteijn et al. 2011), we speculate that Ψ_{lethal} is linked with structural features. *Acer pseudoplatanus* and *C. avellana* have relatively large leaves (leaf area was 116.80 ± 40 and 59.48 ± 23.47 cm², respectively) compared with the other species investigated, which also results in their lower Huber values. These characters could be associated with the less negative Ψ_{lethal} values in both species. Nevertheless, the lack of a significant correlation between Ψ_{lethal} and P_{99} suggests that either additional factors may affect Ψ_{lethal} or that our experimental approach was not sufficiently accurate.

In general, the technique applied to estimate Ψ_{lethal} provides a laborious and time-consuming approach, which has several shortcomings (Figure 3). One of the main problems concerns the intraspecific variation in the recovery rates measured, which could be explained by differences in the microclimate during recovery. For instance, one seedling of *F. excelsior* that was stressed to -2.65 MPa recovered to more than half of the $g_{s \text{ max}}$ overnight upon rewatering under a midday temperature of 20.5 °C and 73% relative air humidity, while another seedling that was stressed to -2.6 MPa required ~ 4 days to recover under warmer midday temperatures (on average 28.25 °C) and drier relative air humidity (on average 46%). This kind of variation could be avoided by working under climate controlled conditions. However, even plants with a similar ψ_m that were recovering under similar vapour pressure deficit levels showed considerable differences in recovery rates. For example, one plant of *C. avellana* that was water-stressed to -2.92 MPa recovered after 11 days to half of the $g_{s \text{ max}}$, while another plant water-stressed to -3 MPa required only 7 days to recover under similar temperature and relative humidity. Additional shortcomings could be that photosynthetic parameters decrease considerably with leaf ageing (Mason et al. 2013, Locke and Ort 2014), which could result in overestimation of Ψ_{lethal} . Moreover, it is possible that water potential measurements of ψ_l and ψ_x become uncoupled during the gradual process of leaf wilting

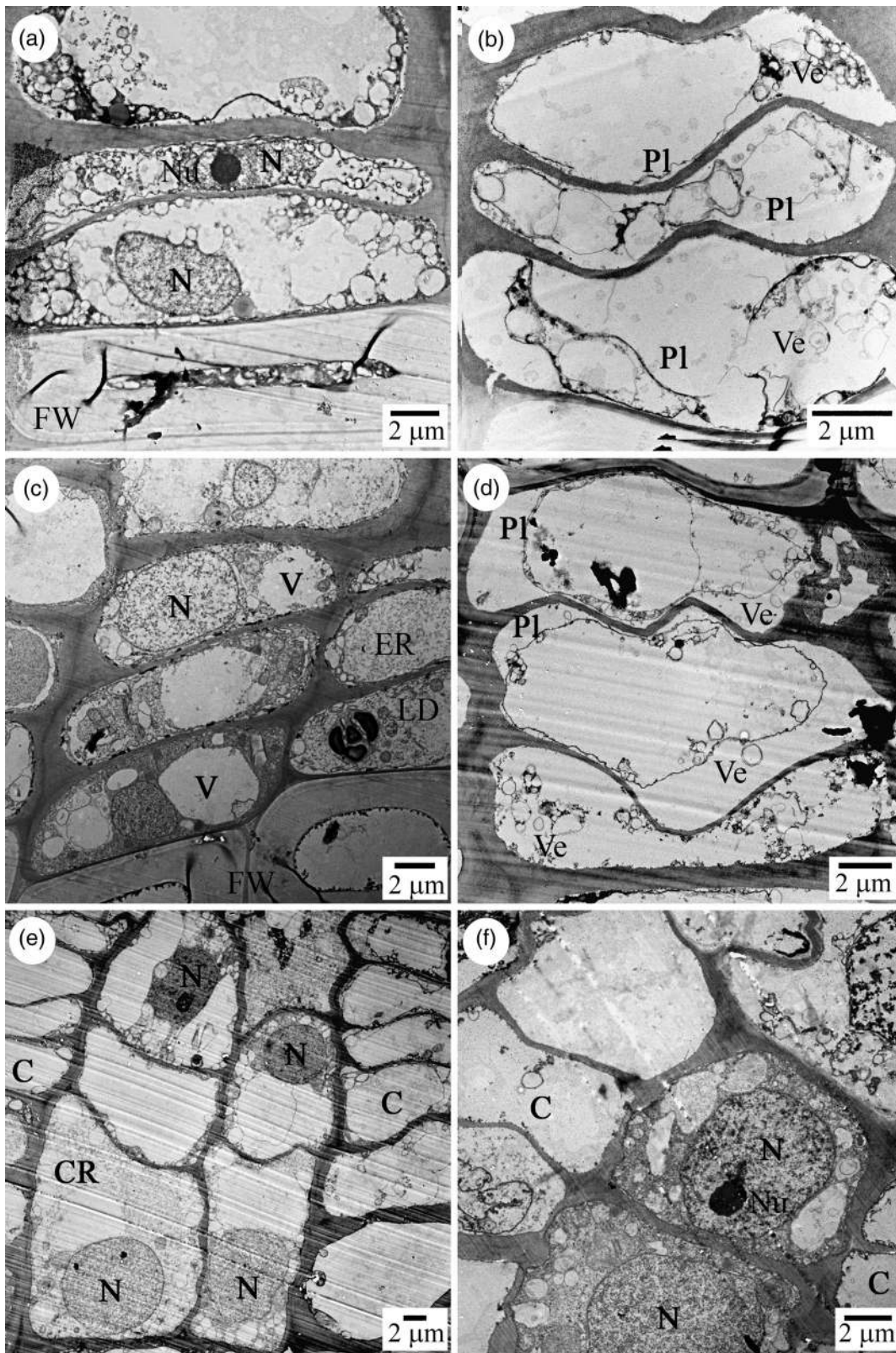


Figure 4. Fusiform cambium cells in transverse stem sections from well-watered (a and c) and severely wilted (b and d) seedlings of *C. avellana* (a and b) and *C. betulus* (c and d). Cambium ray initials in stem (e) and root (f) of severely stressed seedlings of *C. betulus*. CR, cambium ray initial; C, fusiform cambium; ER, endoplasmic reticulum; FW, fibre wall; LD, lipid droplet; N, nucleus; Nu, nucleolus; Pl, plasmalemma; Ve, vesicle; V, vacuole.

and die back, even after bagging up leaves to take water potential measurements.

Several seedlings of *F. excelsior* showed a surprisingly fast recovery after severe water stress levels (Figure 3d). An explanation for the quick recovery is that this species has a relatively large pith (accounting for ~20% of the stem surface area), which could function as hydraulic capacitance tissue during drought stress. We did not find positive root pressure in this species (Cochard et al. 1997), which could also promote fast recovery by refilling embolized conduits. Moreover, *F. excelsior* is the only ring-porous species among the five tree species, which has long and large early wood vessels (maximum vessel diameter = 71 μm). These long and wide vessels might contribute to its high ability to absorb water even under dry soil conditions (Köcher et al. 2009). In addition, active osmotic adjustment of leaf tissue in *F. excelsior* may facilitate the large recovery of gas exchange upon rewatering (Guicherd et al. 1993).

Acer pseudoplatanus and *C. avellana* can be regarded as isohydric plants, while the other three species studied are more anisohydric. However, this classification might be arbitrary because no clear divergences emerged across 70 woody species due to a continuum in leaf gas exchange response to drought. Accordingly, the water potential at 50% of the maximum stomatal conductance (Ψ_{gs50}) was proposed as a quantitative indicator between species (Klein 2014). Indeed, both Ψ_{gs50} and S_{gs50} values among the five species studied show a continuum in stomatal behaviour, with isohydric and anisohydric as two extremes.

Isohydric plants are found to be more vulnerable to xylem embolism, as well as being more commonly distributed in moist habitats, compared with anisohydric plants (Vogt 2001, Meinzer and McCulloh 2013). As embolism resistance is a criterion to evaluate the drought resistance of plants, a close and strong relationship between drought resistance and stomatal control behaviour is likely to occur. Our results are consistent with this hypothesis, as the two isohydric species were the most vulnerable species to xylem embolism, and also are more vulnerable to drought, i.e., it took *A. pseudoplatanus* and *C. avellana* ~14 days of drought stress to reach their lethal water potential. The anisohydric species, however, showed more negative P_{50} and Ψ_{lethal} values, and were more resistant to water stress: Ψ_{lethal} values in *F. excelsior*, *A. campestre* and *C. betulus* required 25, 47 and 53 days of drought stress, respectively.

A 1 : 1 relationship between stomatal closure and stem embolism onset was observed among the five species (Figure 1f), which demonstrates the physiological integration between stems and leaves (Cochard et al. 2002, Ennajeh et al. 2008). In addition, it reflects the sophisticated stomatal regulation strategy, which is also affected by many other factors, such as ABA concentration (Brodribb et al. 2014, Mcadam and Brodribb 2015) and vapour pressure deficit (Will et al. 2013). Although

leaf turgor appears to be an important parameter in plant drought tolerance and plasticity at a global scale (Bartlett et al. 2012, 2014), we did not find a relationship between π_{tip} and P_{50} for the five species studied. The positive but non-significant correlation between π_{tip} and $\Psi_{gs\ e}$, and between π_{tip} and Ψ_{gs50} (Figure 2; Brodribb et al. 2003) is obvious considering that stomatal guard cells need to maintain turgor for stomatal opening.

The cambium ultrastructure of the water-stressed plants can be described as necrosis (van Doorn et al. 2011), with rupture of the plasma membrane and the lack of a vacuole and protoplast (Figure 4b and d) as typical characters. We observed total fusiform cambium failure at the cell level in *C. avellana*, while 90% cellular failure occurred in the more drought resistant *C. betulus*, suggesting that the ~1 month of drought stress did not result in a similar level of death. Similar cellular patterns were described at four different stages of mortality for the root apical meristem in *Arabidopsis* (Duan et al. 2010). Since cambium is one of the most resistant tissues of the plant to drought stress (Barigah et al. 2013b), visualization of cambium breakdown can be used as a method to determine plant death (Figure 4). We also suggest that the gradual changes in cambial cell death can be used to characterize different stages of plant death (Duan et al. 2010).

Ray cells are responsible for transport of water and nutrients in a radial direction, connecting phloem with xylem parenchyma via ray initial cells (Samuels et al. 2006, Plavcová and Jansen 2015). The higher resistance of the ray initial cells to drought-induced necrosis in roots of *C. betulus* compared with the fusiform cambium cells (Figure 4e and f) could be explained by cytoplasmic connection of the ray initial cells with xylem and phloem ray cells. It is known that this symplastic pathway is important for water and carbon reserves (Chaffey and Barlow 2001, Sokołowska and Zagórska-Marek 2012, Spicer 2014, Pfautsch et al. 2015). Therefore, vitality and connectivity of ray parenchyma cells in the wood could play a role in plant survival (Morris et al. 2015). Nevertheless, data on ray cell death are rare. Nakaba et al. (2006) reported that xylem ray parenchyma remained living between 3 and 10 years in *Abies sachalinensis*, with the upper and lower radial cells showing less symplastic connectivity and faster death than the central ray cells.

In conclusion, our results demonstrated that in the five angiosperm tree species studied, Ψ_{lethal} based on photosynthetic recovery time was close to stem P_{99} . During the next spring, however, recovery of plants that passed the estimated Ψ_{lethal} suggests that the method applied is probably underestimating the true Ψ_{lethal} values. This finding also suggests that 100% PLC may not necessarily equal plant death in angiosperm seedlings. Further research on the drought tolerance of meristematic tissues such as cambium could provide an alternative method to predict and define more precisely the point of no recovery and Ψ_{lethal} .

Supplementary data

Supplementary data for this article are available at *Tree Physiology* Online.

Acknowledgments

We thank the Botanical Garden and the Electron Microscopy Section of Ulm University for technical support. Peter Zindl and Jan Plavec are acknowledged for constructing the rainout shelter. We also appreciate help from Sara Ghiasi, Neda Aničić and Vesna Kandić with the field experiment. Many thanks to Dr Fenghui Yuan, Dr Lenka Plavcová, Matthias Klepsch, Hans Malchus, Gabriele Wiest-Danner, Ellen Salzer and Marco Schmitt for assistance in the lab. S.L. acknowledges financial support from the China Scholarship Council (CSC), and assistance for statistical analysis from Yujun Li.

Conflict of interest

None declared.

References

- Abe H, Nakai T, Utsumi Y, Kagawa A (2003) Temporal water deficit and wood formation in *Cryptomeria japonica*. *Tree Physiol* 23:859–863.
- Anderegg WRL (2015) Spatial and temporal variation in plant hydraulic traits and their relevance for climate change impacts on vegetation. *New Phytol* 205:1008–1014.
- Balducci L, Deslauriers A, Giovannelli A, Rossi S, Rathgeber CBK (2013) Effects of temperature and water deficit on cambial activity and woody ring features in *Picea mariana* saplings. *Tree Physiol* 33:1006–1017.
- Barigah TS, Charrier O, Douris M, Bonhomme M, Herbette S, Améglio T, Fichot R, Brignolas F, Cochard H (2013a) Water stress-induced xylem hydraulic failure is a causal factor of tree mortality in beech and poplar. *Ann Bot* 112:1431–1437.
- Barigah TS, Bonhomme M, Lopez D, Traore A, Douris M, Venisse JS, Cochard H, Badel E (2013b) Modulation of bud survival in *Populus nigra* sprouts in response to water stress-induced embolism. *Tree Physiol* 33:261–274.
- Bartlett MK, Scoffoni C, Sack L (2012) The determinants of leaf turgor loss point and prediction of drought tolerance of species and biomes: a global meta-analysis. *Ecol Lett* 15:393–405.
- Bartlett MK, Zhang Y, Kreidler N, Sun S, Ardy R, Cao K, Sack L (2014) Global analysis of plasticity in turgor loss point, a key drought tolerance trait. *Ecol Lett* 17:1580–1590.
- Bond BJ, Kavanagh KL (1999) Stomatal behavior of four woody species in relation to leaf-specific hydraulic conductance and threshold water potential. *Tree Physiol* 19:503–510.
- Brodribb TJ (2009) Xylem hydraulic physiology: the functional backbone of terrestrial plant productivity. *Plant Sci* 177:245–251.
- Brodribb TJ, Cochard H (2009) Hydraulic failure defines the recovery and point of death in water-stressed conifers. *Plant Physiol* 149:575–584.
- Brodribb TJ, Holbrook NM (2004) Stomatal protection against hydraulic failure: a comparison of coexisting ferns and angiosperms. *New Phytol* 162:663–670.
- Brodribb TJ, Holbrook NM, Edwards EJ, Gutiérrez MV (2003) Relations between stomatal closure, leaf turgor and xylem vulnerability in eight tropical dry forest trees. *Plant Cell Environ* 26:443–450.
- Brodribb TJ, Bowman DJMS, Nichols S, Delzon S, Burrell R (2010) Xylem function and growth rate interact to determine recovery rates after exposure to extreme water deficit. *New Phytol* 188:533–542.
- Brodribb TJ, McAdam SAM, Jordan GJ, Martins SCV (2014) Conifer species adapt to low-rainfall climates by following one of two divergent pathways. *Proc Natl Acad Sci USA* 111:14489–14493.
- Cai J, Li S, Zhang H, Zhang S, Tyree MT (2014) Recalcitrant vulnerability curves: methods of analysis and the concept of fibre bridges for enhanced cavitation resistance. *Plant Cell Environ* 37:35–44.
- Carnicer J, Barbata A, Sperlich D, Coll M, Peñuelas J (2013) Contrasting trait syndromes in angiosperms and conifers are associated with different responses of tree growth to temperature on a large scale. *Front Plant Sci* 4:409. doi:10.3389/fpls.2013.00409
- Chaffey N, Barlow P (2001) The cytoskeleton facilitates a three-dimensional symplasmic continuum in the long-lived ray and axial parenchyma cells of angiosperm trees. *Planta* 213:811–823.
- Chen JW, Zhang Q, Li XS, Cao KF (2010) Gas exchange and hydraulics in seedlings of *Hevea brasiliensis* during water stress and recovery. *Tree Physiol* 30:876–885.
- Choat B, Sack L, Holbrook NM (2007) Diversity of hydraulic traits in nine *Cordia* species growing in tropical forests with contrasting precipitation. *New Phytol* 175:686–698.
- Choat B, Jansen S, Brodribb TJ et al. (2012) Global convergence in the vulnerability of forests to drought. *Nature* 491:752–755.
- Cochard H, Peiffer M, Gall KL, André G (1997) Developmental control of xylem hydraulic resistances and vulnerability to embolism in *Fraxinus excelsior* L.: impacts on water relations. *J Exp Bot* 48:655–663.
- Cochard H, Coll L, Le Roux X, Améglio T (2002) Unraveling the effects of plant hydraulics on stomatal closure during water stress in walnut. *Plant Physiol* 128:282–290.
- Cochard H, Damour G, Bodet C, Tharwat I, Poirier M, Améglio T (2005) Evaluation of a new centrifuge technique for rapid generation of xylem vulnerability curves. *Physiol Plant* 124:410–418.
- Cochard H, Barigah ST, Kleinhentz M, Eshel A (2008) Is xylem cavitation resistance a relevant criterion for screening drought resistance among *Prunus* species? *J Plant Physiol* 165:976–982.
- Cochard H, Badel E, Herbette S, Delzon S, Choat B, Jansen S (2013) Methods for measuring plant vulnerability to cavitation: a critical review. *J Exp Bot* 64:4779–4791.
- de Luis M, Novak K, Raventós J, Gričar J, Prisljan P, Čufar K (2011) Cambial activity, wood formation and sapling survival of *Pinus halepensis* exposed to different irrigation regimes. *For Ecol Manag* 262:1630–1638.
- Dixon HH, Joly J (1895) The path of the transpiration-current. *Ann Bot* 9:403–420.
- Duan Y, Zhang W, Li B, Wang Y, Li K, Sodmergen, Han C, Zhang Y, Li X (2010) An endoplasmic reticulum response pathway mediates programmed cell death of root tip induced by water stress in *Arabidopsis*. *New Phytol* 186:681–695.
- Ennajeh M, Tounekti T, Vadel AM, Khemira H, Cochard H (2008) Water relations and drought-induced embolism in olive (*Olea europaea*) varieties 'Meski' and 'Chemlali' during severe drought. *Tree Physiol* 28:971–976.
- Farrar JJ, Evert RF (1997) Ultrastructure of cell division in the fusiform cells of the vascular cambium of *Robinia pseudoacacia*. *Trees* 11:203–215.
- Fuchs M, van Bel AJE, Ehlers K (2010) Season-associated modifications in symplasmic organization of the cambium in *Populus nigra*. *Ann Bot* 105:375–387.
- Gričar J, Jagodic Š, Šefc B, Trajković J, Eler K (2014) Can the structure of dormant cambium and the widths of phloem and xylem increments be used as indicators for tree vitality? *Eur J For Res* 133:551–562.
- Griffiths CA, Gaff DF, Neale AD (2014) Drying without senescence in resurrection plants. *Front Plant Sci* 5:36. doi:10.3389/fpls.2014.00036
- Guicherd P, Peltier JP, Gout E, Bligny R, Marigo G (1993) Osmotic adjustment in *Fraxinus excelsior* L.: malate and mannitol accumulation in leaves under drought conditions. *Trees* 11:155–161.

- Hartmann H, Adams HD, Anderegg WRL, Jansen S, Zeppel MJB (2015) Research frontiers in drought-induced tree mortality: crossing scales and disciplines. *New Phytol* 205:965–969.
- Hoffmann WA, Marchin RM, Abit P, Lau OL (2011) Hydraulic failure and tree dieback are associated with high wood density in a temperate forest under extreme drought. *Glob Change Biol* 17:2731–2742.
- Hubbard RM, Ryan MG, Stiller V, Sperry JS (2001) Stomatal conductance and photosynthesis vary linearly with plant hydraulic conductance in ponderosa pine. *Plant Cell Environ* 24:113–121.
- Klein T (2014) The variability of stomatal sensitivity to leaf water potential across tree species indicates a continuum between isohydric and anisohydric behaviours. *Funct Ecol* 28:1313–1320.
- Köcher P, Gebauer T, Horna V, Leuschner C (2009) Leaf water status and stem xylem flux in relation to soil drought in five temperate broad-leaved tree species with contrasting water use strategies. *Ann For Sci* 66:101. doi:10.1051/forest/2008076
- Kumagai T, Porporato A (2012) Strategies of a Bornean tropical rainforest water use as a function of rainfall regime: isohydric or anisohydric? *Plant Cell Environ* 35:61–71.
- Kursar TA, Engelbrecht BMJ, Burke A, Tyree MT, El Omari B, Giraldo JP (2009) Tolerance to low leaf water status of tropical tree seedlings is related to drought performance and distribution. *Funct Ecol* 23:93–102.
- Lens F, Sperry JS, Christman MA, Choat B, Rabaey D, Jansen S (2011) Testing hypotheses that link wood anatomy to cavitation resistance and hydraulic conductivity in the genus *Acer*. *New Phytol* 190:709–723.
- Liphshitz N, Lev-Yadun S (1986) Cambial activity of evergreen and seasonal dimorphics around the Mediterranean. *IAWA J* 7:145–153.
- Locke AM, Ort DR (2014) Leaf hydraulic conductance declines in coordination with photosynthesis, transpiration and leaf water status as soybean leaves age regardless of soil moisture. *J Exp Bot* 65:6617–6627.
- Lopez OR, Kursar TA, Cochard H, Tyree MT (2005) Interspecific variation in xylem vulnerability to cavitation among tropical tree and shrub species. *Tree Physiol* 25:1553–1562.
- Lu Y, Equiza MA, Deng X, Tyree MT (2010) Recovery of *Populus tremuloides* seedlings following severe drought causing total leaf mortality and extreme stem embolism. *Physiol Plant* 140:246–257.
- Manzoni S, Vico G, Katul G, Palmroth S, Porporato A (2014) Optimal plant water-use strategies under stochastic rainfall. *Water Resour Res* 50:5379–5394.
- Markesteyn L, Poorter L, Paz H, Sack L, Bongers F (2011) Ecological differentiation in xylem cavitation resistance is associated with stem and leaf structural traits. *Plant Cell Environ* 34:137–148.
- Martorell S, Diaz-Espejo A, Medrano H, Ball MC, Choat B (2014) Rapid hydraulic recovery in *Eucalyptus pauciflora* after drought: linkages between stem hydraulics and leaf gas exchange. *Plant Cell Environ* 37:617–626.
- Mason CM, McGaughey SE, Donovan LA (2013) Ontogeny strongly and differentially alters leaf economic and other key traits in three diverse *Helianthus* species. *J Exp Bot* 64:4089–4099.
- McAdam SAM, Brodribb TJ (2015) Hormonal dynamics contributes to divergence in seasonal stomatal behaviour in a monsoonal plant community. *Plant Cell Environ* 38:423–432.
- Meinzer FC, McCulloh KA (2013) Xylem recovery from drought-induced embolism: where is the hydraulic point of no return? *Tree Physiol* 33:331–334.
- Meinzer FC, Johnson DM, Lachenbruch B, McCulloh KA, Woodruff DR (2009) Xylem hydraulic safety margins in woody plants: coordination of stomatal control of xylem tension with hydraulic capacitance. *Funct Ecol* 23:922–930.
- Miyashita K, Tanakamaru S, Maitani T, Kimura K (2005) Recovery responses of photosynthesis, transpiration, and stomatal conductance in kidney bean following drought stress. *Environ Exp Bot* 53:205–214.
- Morris H, Plavcová L, Cvecko P et al. (2015) A global analysis of parenchyma tissue fractions in secondary xylem of seed plants. *New Phytol* (in press).
- Nakaba S, Sano Y, Kubo T, Funada R (2006) The positional distribution of cell death of ray parenchyma in a conifer, *Abies sachalinensis*. *Plant Cell Rep* 25:1143–1148.
- Nardini A, Tyree MT, Salleo S (2001) Xylem cavitation in the leaf of *Prunus laurocerasus* and its impact on leaf hydraulics. *Plant Physiol* 125:1700–1709.
- Nardini A, Battistuzzo M, Savi T (2013) Shoot desiccation and hydraulic failure in temperate woody angiosperms during an extreme summer drought. *New Phytol* 200:322–329.
- Ogasa M, Miki NH, Murakami Y, Yoshikawa K (2013) Recovery performance in xylem hydraulic conductivity is correlated with cavitation resistance for temperate deciduous tree species. *Tree Physiol* 33:335–344.
- Pfautsch S, Renard J, Tjoelker MG, Salih A (2015) Phloem as capacitor: radial transfer of water into xylem of tree stems occurs via symplastic transport in ray parenchyma. *Plant Physiol* 167:963–971.
- Pineda-García F, Paz H, Meinzer FC (2013) Drought resistance in early and late secondary successional species from a tropical dry forest: the interplay between xylem resistance to embolism, sapwood water storage and leaf shedding. *Plant Cell Environ* 36:405–418.
- Plavcová L, Jansen S (2015) The role of xylem parenchyma in the storage and utilization of non-structural carbohydrates. In: Hacke UG (ed.) *Functional and ecological xylem anatomy*. Springer, Heidelberg, pp 209–234.
- Poorter H, Bühler J, van Dusschoten D, Climent J, Postma JA (2012) Pot size matters: a meta-analysis of the effects of rooting volume on plant growth. *Funct Plant Biol* 39:839–850.
- Rossi S, Simard S, Rathgeber CBK, Deslauriers A, De Zan C (2009a) Effects of a 20-day-long dry period on cambial and apical meristem growth in *Abies balsamea* seedlings. *Trees* 23:85–93.
- Rossi S, Simard S, Deslauriers A, Morin H (2009b) Wood formation in *Abies balsamea* seedlings subjected to artificial defoliation. *Tree Physiol* 29:551–558.
- Rossi S, Anfodillo T, Cufar K et al. (2013) A meta-analysis of cambium phenology and growth: linear and non-linear patterns in conifers of the northern hemisphere. *Ann Bot* 112:1911–1920.
- Sack L, Pasquetl-Kok J. Leaf pressure-volume curve parameters. <http://prometheuswiki.publish.csiro.au/tiki-index.php?page=Leaf+pressure+volume+curve+parameters> (19 March 2015, date last accessed).
- Sade N, Gebremedhin A, Moshelion M (2012) Risk-taking plants: anisohydric behavior as a stress-resistance trait. *Plant Signal Behav* 7:767–770.
- Salleo S, Nardini A, Pitt F, Lo Gullo MA (2000) Xylem cavitation and hydraulic control of stomatal conductance in Laurel (*Laurus nobilis* L.). *Plant Cell Environ* 23:71–79.
- Samuels AL, Kaneda M, Rensing KH (2006) The cell biology of wood formation: from cambial divisions to mature secondary xylem. *Can J Bot* 84:631–639.
- Scholz A, Rabaey D, Stein A, Cochard H, Smets E, Jansen S (2013) The evolution and function of vessel and pit characters with respect to cavitation resistance across 10 *Prunus* species. *Tree Physiol* 33:684–694.
- Scholz FG, Bucci SJ, Goldstein G (2014) Strong hydraulic segmentation and leaf senescence due to dehydration may trigger die-back in *Nothofagus dombeyi* under severe droughts: a comparison with the co-occurring *Austrocedrus chilensis*. *Trees* 28:1475–1487.
- Sokolowska K, Zagórska-Marek B (2012) Symplasmic, long-distance transport in xylem and cambial regions in branches of *Acer pseudo-platanus* (Aceraceae) and *Populus tremula* × *P. tremuloides* (Salicaceae). *Am J Bot* 99:1745–1755.
- Sparks JP, Black RA (1999) Regulation of water loss in populations of *Populus trichocarpa*: the role of stomatal control in preventing xylem cavitation. *Tree Physiol* 19:453–459.
- Sperry JS (2000) Hydraulic constraints on plant gas exchange. *Agric For Meteorol* 104:13–23.

- Sperry JS, Pockman WT (1993) Limitation of transpiration by hydraulic conductance and xylem cavitation in *Betula occidentalis*. *Plant Cell Environ* 16:279–287.
- Spicer R (2014) Symplasmic networks in secondary vascular tissues: parenchyma distribution and activity supporting long-distance transport. *J Exp Bot* 65:1829–1848.
- Tardieu F, Simonneau T (1998) Variability among species of stomatal control under fluctuating soil water status and evaporative demand: modelling isohydric and anisohydric behaviours. *J Exp Bot* 49:419–432.
- Thomas H (2013) Senescence, ageing and death of the whole plant. *New Phytol* 197:696–711.
- Torres-Ruiz JM, Jansen S, Choat B et al. (2015) Direct X-ray microtomography observation confirms the induction of embolism upon xylem cutting under tension. *Plant Physiol* 167:40–43.
- Tyree MT (2003a) Plant hydraulics: the ascent of water. *Nature* 423:923. doi:10.1038/423923a
- Tyree MT (2003b) Hydraulic limits on tree performance: transpiration, carbon gain and growth of trees. *Trees* 17:95–100.
- Tyree MT, Ewers FW (1991) The hydraulic architecture of trees and other woody plants. *New Phytol* 119:345–360.
- Tyree MT, Sperry JS (1988) Do woody plants operate near the point of catastrophic xylem dysfunction caused by dynamic water stress? Answers from a model. *Plant Physiol* 88:574–580.
- Tyree MT, Patiño S, Becker P (1998) Vulnerability to drought-induced embolism of Bornean heath and dipterocarp forest trees. *Tree Physiol* 18:583–588.
- Tyree MT, Vargas G, Engelbrecht BM, Kursar TA (2002) Drought until death do us part: a case study of the desiccation-tolerance of a tropical moist forest seedling-tree, *Licania platypus* (Hemsl.) Fritsch. *J Exp Bot* 53:2239–2247.
- Tyree MT, Engelbrecht BM, Vargas G, Kursar TA (2003) Desiccation tolerance of five tropical seedlings in Panama. Relationship to a field assessment of drought performance. *Plant Physiol* 132:1439–1447.
- Urli M, Porté AJ, Cochard H, Guengant Y, Burlett R, Delzon S (2013) Xylem embolism threshold for catastrophic hydraulic failure in angiosperm trees. *Tree Physiol* 33:672–683.
- van Doorn WG, Beers EP, Dangi JL et al. (2011) Morphological classification of plant cell deaths. *Cell Death Differ* 18:1241–1246.
- Vogt UK (2001) Hydraulic vulnerability, vessel refilling, and seasonal courses of stem water potential of *Sorbus aucuparia* L. and *Sambucus nigra* L. *J Exp Bot* 52:1527–1536.
- Wang R, Zhang L, Zhang S, Cai J, Tyree MT (2014) Water relations of *Robinia pseudoacacia* L.: Do vessels cavitate and refill diurnally or are R-shaped curves invalid in *Robinia*? *Plant Cell Environ* 37:2667–2678.
- Wheeler JK, Huggett BA, Tofte AN, Rockwell FE, Holbrook NM (2013) Cutting xylem under tension or supersaturated with gas can generate PLC and the appearance of rapid recovery from embolism. *Plant Cell Environ* 36:1938–1949.
- Will RE, Wilson SM, Zou CB, Hennessey TC (2013) Increased vapor pressure deficit due to higher temperature leads to greater transpiration and faster mortality during drought for tree seedlings common to the forest-grassland ecotone. *New Phytol* 200:366–374.